Preprints of the 8th IFAC Symposium on Fault Detection, Supervision and Safety of Technical Processes (SAFEPROCESS) August 29-31, 2012. Mexico City, Mexico

An experimentally validated capacity degradation model for Li-ion batteries in PHEVs applications

Fabio Todeschini [*,1], **Simona Onori** [**,2], **Giorgio Rizzoni** [**,***]

[*] *Department of Electronics and Computer Engineering, Politecnico di Milano, Milan, Italy*
[**] *Center for Automotive Research, The Ohio State University, Columbus, OH, USA*
[***] *Department of Mechanical and Aerospace Engineering, The Ohio State University, Columbus, OH,USA*

Abstract: This paper proposes an experimentally validated capacity degradation model for Li-Ion batteries deployed in plug-in hybrid electric vehicle (PHEV) applications. An aging and characterization campaign aimed to mimic the real battery usage at low state of charge during charge sustaining operation was conducted on six Lithium iron phosphate (LiFePO4) battery cells. We present an analytical model, driven by experimental data, that relates the main aging factors under which the battery cells have been tested to capacity fade. State-of-health (SOH) and prediction of battery end-of-life (EOL) algorithms can be designed with the proposed model.

Keywords: Li-Ion battery; Aging and characterization experiments; Capacity degradation model; Automotive.

1. INTRODUCTION

Vehicle electrification is one of the key thrusts of the automotive industry today, driven by the goal to reduce dependence on petroleum and CO2 emissions. the heart of an electrified vehicle is the battery, and today electrochemical energy storage is the single most important barrier to the widespread introduction on electrified vehicles, whether pure EVs plug-in hybrids (PHEVs) or hybrids (HEVs), because of the life cycle cost of battery systems. Understanding aging phenomena in batteries is an important step towards reducing the cost of such energy storage solutions in vehicles.

Among different battery chemistries, Li-ion based batteries are today regarded as the most suitable technology for hybrid and electric vehicles applications as they offer greater power and energy density compared to the other available battery chemistries, at least in the short and medium term. Although Li-ion batteries technology seems to be most suitable to better exploit all the advantages of powertrain electrification, there are many aspects of this technology that need to be improved before significant PHEV and EV market penetration becomes possible. Key issues are: battery cost, life, safety, and reliability. In particular, a deeper understanding of battery aging will provide key insights useful to improve the longevity and reliability of batteries.

Batteries age with use (Vetter et al. [2005], Schmidt et al. [2010], Onori et al. [2011]) and battery aging manifests itself through capacity loss and internal resistance increasing, which, in turn, cause faster temperature rise in operation, reduced charge acceptance, lower voltage, and increased self-discharge. Much research has been carried out to estimate those effects in batteries used in automotive applications (Saha and Goebel [2009], Rubagotti et al. [2009], Plett [2005], Plett [2004], X. Tang [2011]). In particular, in this work we focus on studying the capacity fade phenomenon in batteries used in PHEV applications. We investigate and model the correlation between the so-called stress factors and the degradation due to the cycle aging for state-of-health assessment, remaining useful life estimation and ultimately battery life extension. Stress factors are factors that characterize the domain of operation of the battery, such as, temperature, state-of-charge, depth of discharge, etc.

The paper is structured as follows. First, we describe an experimental aging campaign conducted at The Ohio State University Center for Automotive Research (OSU-CAR) to replicate battery usage in charge-sustaining operation in a PHEV, that is when the PHEV has depleted much of the stored charge after providing EV range. The aging results are presented in Section 2. Next, aging data is used to develop a capacity degradation model that is presented and validated in Section 3 and Section 4. Finally, in Section 5 we present some remarks and propose future work to conclude the paper.

[1] Fabio Todeschini conducted this work while he was a visiting scholar at the Center for Automotive Research The Ohio State University.

[2] Corresponding author {e-mail: onori.1@osu.edu}.

Fig. 1. A123 Lithium iron phosphate (LiFePO4) battery cell.

Table 1. Summary of aging campaign.

i	$C_{rate}\,[\frac{1}{h}]$	$\underline{SOC}\,[\%]$	$\overline{SOC}\,[\%]$	$T_c\,[\frac{min}{cycle}]$	$Ah_c\,[\frac{Ah}{cycle}]$
#1	2	0	10	6	0.46
#2	4	0	10	3	0.46
#3	8	0	10	1.5	0.46
#4	2	0	30	18	1.38
#5	4	0	30	9	1.38
#6	8	0	30	4.5	1.38

2. AGING CAMPAIGN EXPERIMENTS

The primary factors that influence battery aging (i.e. stress factors) in PHEV applications are described in Onori et al. [2012], Laboratory [2010]). They are:

- ΔSOC: State of Charge (SOC) range in which the battery works;
- C_{rate}: Current severity defined as:

$$C_{rate} = \frac{I}{Q_n} \tag{1}$$

  where I is the current and Q_n is the nominal battery capacity;
- T: battery skin temperature.

To understand how the aging process is affected by the stress factors, an aging campaign was conducted on a set of A123 ANR26650 cylindrical Li-Ion Cells (Fig. 1) at OSU-CAR. The battery cell characteristics are as follows:

- Nominal capacity: $Q_n = 2.3\,Ah$
- Nominal Voltage: $V_n = 3.3\,V$
- Max continuous discharge current $I_{max,c} = 70\,A$
- Operative Temperature: $T_{op} = -30^\circ\,C \div 60^\circ\,C$

Each cell was aged under different load conditions that consisted of varying the (C_{rate}) and SOC range ($\Delta SOC = \overline{SOC} - \underline{SOC}$) at a fixed temperature of $55°C$. The aging temperature of $55°C$ was chosen to accelerate the aging experiments. These conditions are summarized in Table 1.

The aging experiments were designed to emulate the charge-sustaining mode of operation in PHEV applications, to understand and ultimately quantify the degradation when the battery operates at low SOC and through a shallow DOD. Starting from $\underline{SOC} = 0\,\%$ [3] each cell was aged up to 10%, 20% and 30% SOC at three different C_{rate}, namely $2C$, $4C$ and $8C$. The design of experiment gives rise to the matrix of 9 experiments summarized in Table 1.

[3] The choice of cycling the battery starting from operating $\underline{SOC} = 0\,\%$ was made to: 1. accelerate the aging; 2. have a more stable way to control the SOC of operation, as the threshold of zero SOC can be determined by simply monitoring the voltage.

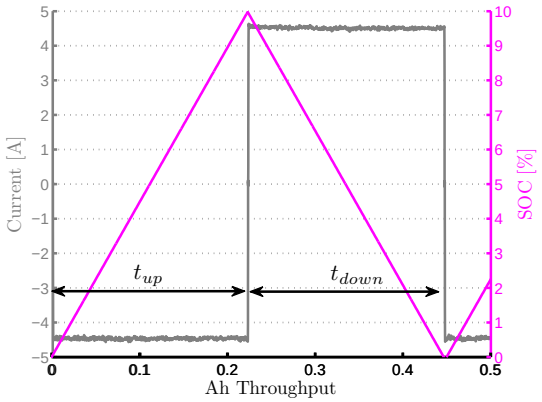

Fig. 2. Zoom of current profile ($C_{rate} \approx 2\,\frac{1}{h}$) and SOC ($\underline{SOC} = 0\,\%$, $\overline{SOC} = 10\,\%$) during experiment #1.

Each battery was aged via a square-wave current profile, which results in triangular SOC profile between $\underline{SOC}$ and $\overline{SOC}$ (Fig. 2), where $\underline{SOC} = 0\%$ and $\overline{SOC}$ is 10%, 20% and 30% SOC, respectively.

Assessments tests were performed periodically during the aging activity of each cells at the same temperature of the aging. These included: capacity tests, electrochemical impedance spectroscopy (EIS) measurements and high-power pulse tests (HPPT) (see Laboratory [2010] for more detail).

In particular, capacity tests were performed by first fully charging the battery at a current rate of $C_{rate} = 1\,\frac{1}{h}$, then, letting the battery rest for an hour, and finally, discharging it at $C_{rate} = 1\,\frac{1}{h}$. Every capacity test was performed at a controlled temperature of $T = 55°C$. The battery capacity under each test condition is calculated according to:

$$Q_i(n_k) = t_{disch} \cdot I_{disch} \tag{2}$$

where t_{disch} and I_{disch} are the discharge time and the discharge current during the capacity test and $Q_i(n_k)$ represents the battery capacity after n_k aging cycles, for the $i-th$ battery cell (see Table 1).

As a new estimate of battery capacity is obtained after each capacity test, the aging cycling profile is periodically updated after each capacity test, and the time interval in which the battery is charged (t_{up}, see Fig. 2) is decided from the most updated capacity experiment as a function of t_{disch}:

$$t_{up,k} = \frac{t_{disch} \cdot \frac{\Delta SOC}{100}}{\frac{I}{I_{nom}}} \tag{3}$$

where ΔSOC and I take values on the given experiment and I_{nom} is the nominal battery current of $2.3\,A$ (corresponding to $C_{rate} = 1\,\frac{1}{h}$).

In summary, the aging protocol for each experiment i consists of the following steps:

1 Perform an initial capacity assessment test on a new battery (the initial capacity $Q(n_0)$ is obtained);
2 Age the battery with the square-wave discharge/charge protocol of Fig. 2. Starting with the battery completely depleted ($0\%SOC$), the battery is charged with a given C_{rate} current for $t_{up,k}$ seconds, until it reaches $\overline{SOC}$ (see Table 1); then the discharge phase

takes place (at the same C_{rate} of the charge phase); when the voltage drops below $2.5\,[V]$ ($0\%SOC$) another aging cycle is executed.

3 Perform periodic assessment tests during the aging to originate new estimates of battery capacity, $Q(n_k)$, as the battery ages. (Note that capacity tests were performed roughly every two weeks).

4 From the newly assessed capacity values $Q(n_k)$ the discharge time t_{disch} is updated, and used in Eq. 3 to compute $t_{up,k}$ which is in turn used in the aging cycling to control the $\overline{SOC}$.

The process described above is repeated for each battery until the end-of-life criterion is reached, which corresponds to a drop in capacity of 20% with respect to its nominal value [4]. A complete aging experiment could last from 3 to 6 months.

During the experiments, current (I), voltage (V) and temperature (T) were acquired with a sample frequency $f_s = 10\,Hz$.

The dark grey curve in Fig. 2 illustrates an aging cycle consisting of a charge current (negative by convention) followed by a (positive) discharge current. The total ampere-hours (Ah) throughput corresponding to each aging cycle is:

$$Ah_c = Q(n_k) \cdot \Delta SOC \cdot 2 \tag{4}$$

where, $Q_i(n_k)$ is the last update of capacity value, and the period (in minutes) each aging cycle lasts is given by:

$$T_c = \frac{Ah_c}{I} \cdot 60 \tag{5}$$

where I is the aging current used for a given experiments. As the battery capacity decreases with aging, the two quantities, Ah_c and T_c, will also decrease over battery lifespan. In the next section, we present the data collected during the aging campaign and propose a new model to predict capacity degradation.

3. EXPERIMENTAL DATA ANALYSIS

Capacity data collected from the 6 battery cells are shown in Fig. 3. The capacity degradation measured after n_k aging cycles for the generic experiment i, is defined as:

$$C_i(n_k) = \frac{Q_i(n_k)}{Q_i(n_0)} \cdot 100 \tag{6}$$

where $Q_i(n_0) = Q_i(0)$ is the measured capacity at beginning of life and the index k indicates the k-th capacity test ($k = 0, \ldots, N$, where N represents the number of capacity points obtained foe each experiments). For instance, the capacity assessed at the first capacity test done after 300 aging cycle for battery cell #2 is:

$$C_2(n_1) = \frac{Q_2(n_1)}{Q_2(n_0)} \cdot 100 \tag{7}$$

with $n_1 = 300$.

The capacity degradation can be correlated to either the total ampere-hours throughput, defined as:

$$Ah(t) = \int_0^t |I(\tau)| d\tau \tag{8}$$

[4] The choice of 20% capacity degradation is in keeping with automotive industry standards, wherein a battery is considered no longer suitable for automotive use when 20% of its life has been depleted.

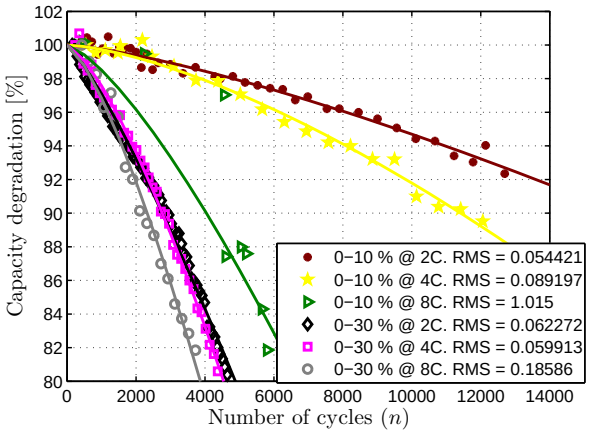

Fig. 3. Capacity points and corresponding fitting curves for the six aging experiments.

or the total number of aging cycles, defined as follows:

$$n = \frac{Ah}{2 \cdot \Delta SOC \cdot Q(n_k)} \tag{9}$$

The one-to-one relationship between total ampere-hours throughput to total number of aging cycle allows to express the capacity degradation either as a function of Ah or as a function of n.

In this work we choose to express capacity degradation as a function of n, using the following power law fitting curve:

$$C_{f,i}(n) = a_i \cdot n^{b_i} \tag{10}$$

where the coefficients a_i and b_i are fitting parameters related for experiment i. This choice is in agreement with the cumulative aging law proposed in Serrao et al. [2009].

The capacity degradation points obtained for each of the six experiments are fitted with the model of Eq. 10 thus obtaining the continuous curves shown in Fig. 3.

The goodness of the fit is evaluated through the root mean square (RMS) error:

$$RMS_i = \sqrt{\sum_{k=0}^{N} (C_i(n_k) - C_{f,i}(n_k))^2} \tag{11}$$

where $C_{f,i}(n_k)$ is the value of the capacity estimated from the fitting data of the i-th battery after n_k aging cycles whereas $C_i(n_k)$ is the actual capacity data point.

The low mean RMS error,

$$RMS = \frac{\sum_{i=1}^{6} RMS_i}{6} = 0.24\,\% \tag{12}$$

shows good performance of the proposed model structure.

As it emerges from Fig. 3, the capacity degradation behavior strongly depends on the way the battery is aged, i.e., C_{rate} and on ΔSOC of operation, and in principle, the fitting parameters will depend on these as well. A closer look at the dependence of the fitting coefficient b_i on the operating conditions shows that the exponent of the power law is practically constant, as one can notice on Fig. 4. For this, an average value of the fitting exponents, i.e., $\overline{b} = (b_1 + b_2 + \ldots + b_6)/N)$ was chosen as exponent of the proposed power law model of Eq. 10 leading to the form:

$$C_{f,i}(n) = a_i \cdot n^{\overline{b}} = a_i \cdot n^{1.36} \tag{13}$$

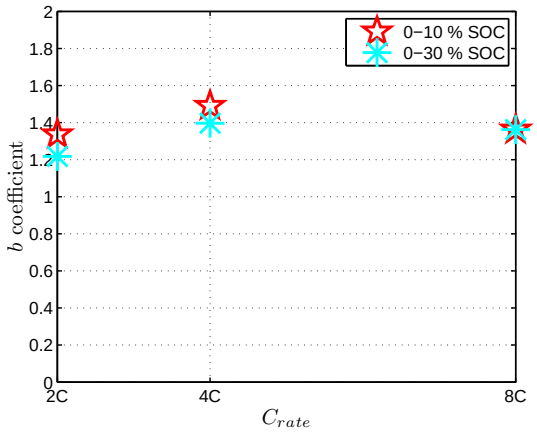

Fig. 4. b_i coefficient values depending on aging factors.

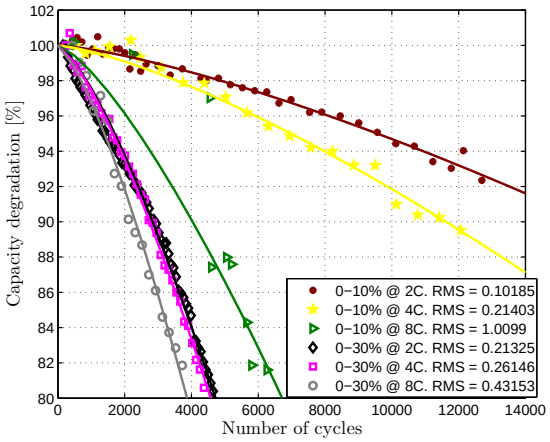

Fig. 5. Capacity points measured in different experiments and $a_i \cdot n^{1.36}$ fitting.

Hence, the model suggested in Eq. 10 indicates that the dependence of capacity degradation on the stress factors is contained in the fitting parameters a_i, as Fig. 6 and Fig. 7 show, where variations of the coefficient a_i are shown as a function of different aging conditions. Moreover, the a_i coefficients represent the initial rate at which the degradation occur as a function of different aging factors.

Figure 6 shows an almost linear trend of coefficients a_i with respect to ΔSOC, while from Fig. 7 the dependency between the coefficient a_i and C_{rate} is such that the higher the C_{rate} the higher the degradation (as one could expect). This latter relationship is modeled through an exponential function.

4. CAPACITY DEGRADATION MODEL

The analysis carried out in the previous section leads to the formulation of the following capacity degradation model:

$$C_{\Delta SOC, C_{rate}}(n) = a(\Delta SOC, C_{rate}) \cdot n^{1.36} = \\ = \left(\alpha + \beta \cdot \Delta SOC + \gamma \cdot e^{C_{rate}}\right) \cdot n^{1.36} \quad (14)$$

which gives the actual capacity value after n aging cycles, knowing the condition at which the battery is operating, namely ΔSOC and C_{rate}. In particular, a least square

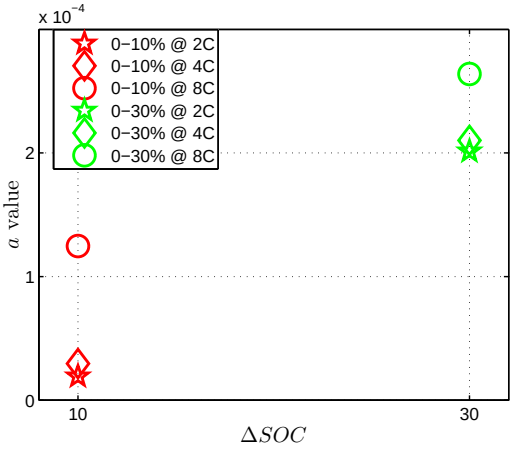

Fig. 6. Coefficient a_i parametrized in terms of C_{rate}.

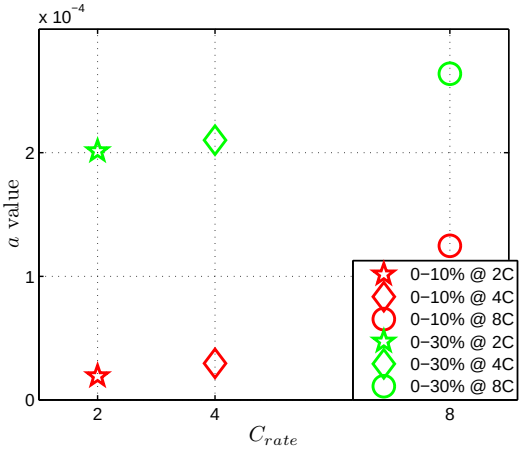

Fig. 7. Coefficient a_i parametrized in terms of ΔSOC.

based optimization study is used to identify the coefficient α, β and γ in the model, which are found to be:

$$\begin{cases} \alpha = -5.31 \cdot 10^{-5} \\ \beta = 8.36 \cdot 10^{-6} \\ \gamma = 2.69 \cdot 10^{-8} \end{cases} \quad (15)$$

The curve fit procedure outlined above results in an rms error of $1.48 \cdot 10^{-5}$.

The fitted surface that expresses the dependence of a_i with respect to ΔSOC and C_{rate} is shown in Fig. 8. This function, named severity factor map is used to quantify the degradation, in terms of capacity decrease, occurring to the battery when the environmental conditions or stress factors are known. It is used in the battery aging model developed in Onori et al. [2012] to predict battery remaining useful life.

5. CONCLUSION

In this paper we have proposed a capacity degradation model for state-of-health assessment in automotive batteries. The model links battery current severity or C_{rate}) and ΔSOC with the capacity degradation behavior. The model obtained can be used for various purposes. For instance:

- It can provide general usage guidelines to minimize battery aging. The model predicts battery degrada-

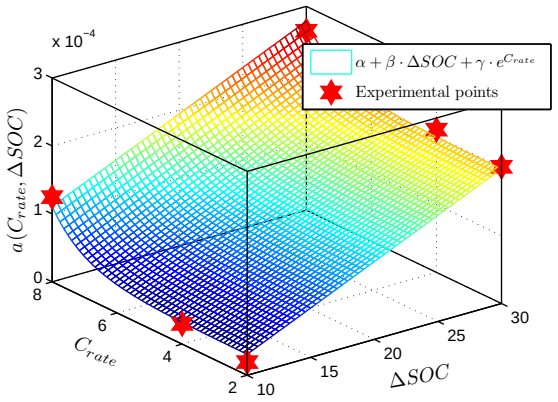

Fig. 8. Aging factor map and a_i coefficient points.

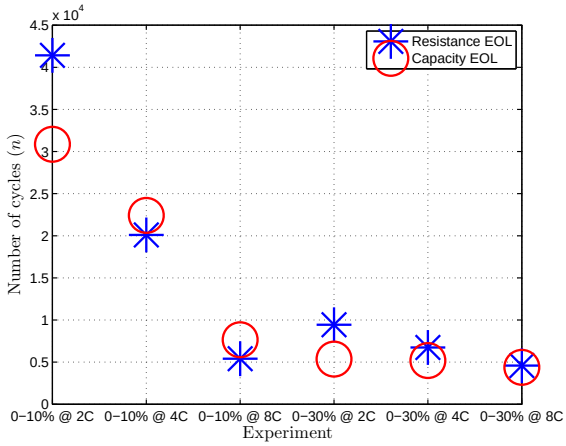

Fig. 9. Resistance EOL and capacity EOL comparison.

tion in charge sustaining mode of operation in PHEV applications.

- Given the knowledge of actual stress factors (which are usually known in automotive applications), the proposed aging model can be used to assess battery state-of-health and predict battery end-of-life.
- the model could also give general usage guidelines for HEV and EV applications. In order to do this, the model should be validated around different SOC ranges, using a similar procedure as that described in this paper.

6. FUTURE WORK

In this work we correlated stress factors to capacity fade. It is well known, though, that aging manifests in batteries in two different ways: power fade and capacity fade. The first one is caused by a resistance increase, the second by a capacity decrease. Capacity fade is the more important effect in PHEVs and EVs applications. This because an aged battery pack cannot store and deliver the energy needed to satisfy the desired electric cruising range.

A similar approach can be adopted to also evaluate changes in resistance due to aging. A procedure for estimating such resistance using measured voltage and current waveforms (Fig. 2) is presented in (Spagnol et al. [2010], Suttman [2011]).

Following the approach used to model capacity fade, one can define battery end of life (EOL) to correspond to a given increase in its internal resistance, for example 100% of its initial value.

A method for incorporating both capacity fade and resistance increase into a single aging index is proposed in Serrao et al. [2009].

Future work will include further investigation of the correlation between capacity fade and resistance increase, to determine whether one of the two factors may be sufficient to estimate battery EOL.

Finally, future work will include temperature effects in the aging model.

ACKNOWLEDGEMENTS

This project was supported in part by the National Science Foundation through CMMI GRANT 0825655 and by the OSU-CAR Industrial Consortium. We are grateful to the NSF and to our industry partners for their generous support.

REFERENCES

Idaho National Laboratory. Battery test manual for plug-in hybrid electric vehicles. *Freedom Car Manual*, 2010.

S. Onori, P. Spagnol, and Y. Guezennec. On-board capacity estimation method for lead-acid battery aging. In *8th International Conference on Lead-Acid Batteries LABAT*, 2011.

S. Onori, P. Spagnol, V. Marano, Y. Guezennec, and G. Rizzoni. A new life estimation method forLithium-ion batteries in Plug-in Hybrid Electric Vehicles applications. *International Journal of Power Electronics*, 4, 2012.

G. L. Plett. Extended kalman filtering for battery management systems of LiPB-based HEV battery packs. part3. state and parameter estimation. *Journal of Power Sources*, 194:277–292, 2004.

G. L. Plett. Dual and joint EKF for simultaneous SOC and SOH estimation. In *Proceedings of the 21st Electric Vehicle Symposium*, 2005.

M. Rubagotti, S. Onori, and G. Rizzoni. Automotive battery prognostics using dual extended kalman filter. 2009.

B. Saha and K. Goebel. Modeling li-ion battery capacity depletion in a particle filtering framework. In *Proceedings of the Annual Conference of the Prognostics and Health Management Society*, 2009.

A. P. Schmidt, M. Bitzer, Á. W. Imre, and L. Guzzella. Model-based distinction and quantification of capacity loss and rate capability fade in li-ion batteries. *Journal of Power Sources*, 195:7634–7638, 2010.

L. Serrao, S. Onori, G. Rizzoni, and Y. Guezennec. A novel model-based algorithm for battery prognosis. In *Proceedings of the 7th IFAC Safeprocess*, 2009.

P. Spagnol, S. Onori, N. Madella, Y. Guezennec, and J. Neal. Aging and characterization of li-ion batteries in a HEV application for lifetime estimation. In

Proceedings of the 6th IFAC Symposium Advances in Automotive Control, 2010.

A. K. Suttman. Lithium ion battery aging experiments and algorithm development for life estimation. Master's thesis, The Ohio State University, Mechanical Engineering, 2011.

J. Vetter, P. Novák, M.R. Wagner, C. Veit, K.C. Möller, J.O. Besenhard, W. Winter, M. Wohlfahrt-Mehrens, C. Vogler, and A. Hammouche. Ageing mechanism in lithium-ion batteries. *Journal of Power Sources*, 147: 269–281, 2005.

J. Lin B. Koch X. Tang, X. mao. Capacity estimation for li-ion batteries. In *Proceedings of the American Control Conference (ACC)*, 2011.